






**Please cite the Published Version**

Ferreira, B , Crapnell, RD , Bernalte, E , Paixão, TRLC  and Banks, CE  (2025) Low-cost conductive polypropylene for electroanalysis in organic solvents using additively manufactured electrodes. *Electrochimica Acta*, 515. 145680 ISSN 0013-4686

**DOI:** <https://doi.org/10.1016/j.electacta.2025.145680>

**Publisher:** Elsevier BV

**Version:** Published Version

**Downloaded from:** <https://e-space.mmu.ac.uk/638231/>

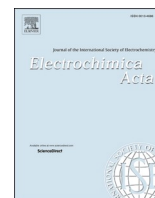
**Usage rights:**  [Creative Commons: Attribution 4.0](https://creativecommons.org/licenses/by/4.0/)

**Additional Information:** This is an open access article which first appeared in *Electrochimica Acta*

**Data Access Statement:** Data will be made available on request.

**Enquiries:**

If you have questions about this document, contact [openresearch@mmu.ac.uk](mailto:openresearch@mmu.ac.uk). Please include the URL of the record in e-space. If you believe that your, or a third party's rights have been compromised through this document please see our Take Down policy (available from <https://www.mmu.ac.uk/library/using-the-library/policies-and-guidelines>)



## Low-cost conductive polypropylene for electroanalysis in organic solvents using additively manufactured electrodes

Bruno Ferreira<sup>a,b</sup>, Robert D. Crapnell<sup>a</sup>, Elena Bernalte<sup>a</sup>, Thiago R.L.C. Paixão<sup>b</sup>,  
Craig E. Banks<sup>a,\*</sup>

<sup>a</sup> Faculty of Science and Engineering, Manchester Metropolitan University, Dalton Building, Chester Street, Manchester M1 5GD, Great Britain

<sup>b</sup> Departamento de Química Fundamental, Instituto de Química, Universidade de São Paulo, São Paulo, SP, 05508-000, Brazil

### ARTICLE INFO

#### Keywords:

Additive manufacturing  
Low-cost  
Electroanalysis  
Non-aqueous electrochemistry  
Organic solvents  
Acetonitrile  
Chlorpromazine

### ABSTRACT

Additive manufacturing electrochemistry allows for the production of bespoke sensing devices, that can be produced rapidly on-site. Through the production of specialised filament, researchers have been able to begin to compete with the electroanalytical performance of classical electrodes, however, only aqueous systems have ever been viable for exploration. In this work, we report the first production of a low material cost poly(propylene) (PP) based conductive filament and its application toward electroanalysis within an organic medium, acetonitrile. By leveraging the chemical stability of PP, alongside the conductive properties of carbon black (CB) and the low-cost nature of graphite (G), high-performance electrodes could be printed at a material cost of less than £0.01 each. The filament containing 20 wt% CB, 20 wt% G and 60 wt% PP was electrochemically characterised, producing a  $k^0$  of  $2.08 (\pm 0.22) \times 10^{-3} \text{ cm s}^{-1}$ . The additive manufactured electrodes were then applied to detect chlorpromazine in acetonitrile, producing a sensitivity of  $51.8 \text{ nA } \mu\text{M}^{-1}$ , limit of detection of  $80 \text{ } \mu\text{M}$  and limit of quantification of  $266 \text{ } \mu\text{M}$ . This work shows how, through the production of bespoke filaments, additive manufacturing electrochemistry can explore new areas of electrochemical research that are currently untapped.

### 1. Introduction

Additive manufacturing electrochemistry is a popular emerging field due to its low-cost of entry, low waste production, high degrees of customisability, and global connectivity. Fused Filament Fabrication (FFF, also known as Fused Deposition Modelling or FDM), is the technique most commonly used in additive manufacturing electrochemistry, primarily due to the low cost and commercial availability of conductive filament. FFF functions through the deposition of thermoplastic material in consecutive, thin-layered cross-sections to build up the final 3-dimensional object. This methodology has been used in work towards sensors [1–5], biosensors [6–8], and energy storage [9–12] using this commercially available filament, with moderate success. FFF has even been used to create accessories [13] and equipment [14] within electrochemical labs. Researchers have spent significant time trying to improve the electrochemical performance of this commercial PLA through various strategies, including optimising the electrode design [15,16], optimising the printing parameters [17–21], or through activating the surface [22–25]. Even so, the final performance of electrodes

printed from this material are substandard and cannot compete with classical commercially available electrodes.

To improve the performance of additively manufactured electrodes, researchers have now taken to making their own bespoke filaments [26]. They have increased levels of conductive filler [27,28], mixed different conductive fillers to maximise performance [29,30] or minimise cost [31,32], and improved the sustainability of materials through using recycled poly(lactic acid) (PLA) [33] or bio-based plasticisers such as castor oil [34]. Although these changes produced large improvements in the conductivities, the inherent problems with using PLA remained, such as its poor chemical stability [35], and the ingress of solution [36] which effectively made all electrodes single use items. To combat this, recent reports have used poly(ethylene terephthalate) (PETg) as the base polymer [37,38]. This removed the issue with solution ingress and made the electrodes reusable, and allowed for different sterilisation methods to be used without affecting the electrochemical performance. Although a significant advancement, the chemical stability of PETg remains an issue [35], limiting the use of these electrodes outside of aqueous or alcoholic solutions.

\* Corresponding author.

E-mail address: [c.banks@mmu.ac.uk](mailto:c.banks@mmu.ac.uk) (C.E. Banks).

<https://doi.org/10.1016/j.electacta.2025.145680>

Received 26 October 2024; Received in revised form 21 December 2024; Accepted 8 January 2025

Available online 9 January 2025

0013-4686/© 2025 The Authors. Published by Elsevier Ltd. This is an open access article under the CC BY license (<http://creativecommons.org/licenses/by/4.0/>).

As such, the use of poly(propylene) (PP) as the base polymer has recently been reported. In the work by Ramos et al. [39] they report the first-time production of a highly electrically conductive additive manufacturing filament containing 40 wt% carbon black (CB). This filament showed resistances on par with the best reports of bespoke conductive PLA without using mixed materials or including any plasticiser compounds. Importantly, this material was shown to be stable within dichloromethane, dimethylformamide and acetonitrile (MeCN) for at least 15 days and was able to perform electrochemical studies within these aprotic environments. [39] The use of PP as the base polymer in filament, therefore, opens the door to organic electroanalysis, an area currently unexplored for additive manufacturing electrochemistry. For the development of electroanalytical sensors there is an important balance between electrochemical performance and cost of production that the platform must strike. As such, simply using CB to induce electrical conductivity is not optimal. It has been reported within PLA previously that graphite (G), a naturally occurring allotrope of carbon, can be used to replace certain proportions of CB within the filament, massively reducing the material cost but, importantly not significantly impacting the electrochemical performance [32].

Consequently, in this work, we propose replacing proportions of the 40 wt% CB used in the previous work with different amounts of graphite to lower the material cost of the filament. We look to optimise this amount in terms of both electrochemical performance and economics. We then aim for the first report on applying additive manufacturing electroanalysis within an organic solvent, opening up this field for researchers to explore.

## 2. Experimental section

### 2.1. Chemicals

All chemicals used throughout this work were used as received without any further purification. All aqueous solutions were prepared with deionised water of a measured resistivity not  $<18.2 \text{ M}\Omega \text{ cm}$  (Milli-Q Integral 3, Watford, UK). Acetonitrile (99.9 %) was purchased from Fisher Scientific (Loughborough, UK). Carbon black was purchased from PI-KEM ( $<20 \text{ nm}$ , Tamworth, UK) and poly(propylene) (PP, Sabic® CX03–81 Natural 00,900) was purchased from Hardie Polymers (Glasgow, UK). Commercial conductive PLA/carbon black filament (1.75 mm, ProtoPasta, Canada) and 3D printing adhesive Magigoo (Thought3D Ltd., Malta) was purchased from Farnell (Leeds, UK). Hexaammineruthenium (III) chloride ( $[\text{Ru}(\text{NH}_3)_6]^{3+}$ , 98 %), potassium ferricyanide (99 %), potassium ferrocyanide (98.5–102 %), sodium hydroxide ( $>98 \%$ ), potassium chloride (99.0–100.5 %), graphite flakes ( $<20 \mu\text{m}$ ), and chlorpromazine (CPZ,  $\geq 98 \%$ ) were purchased from Merck (Gillingham, UK).

### 2.2. Filament production and additive manufacturing of the electrodes

Please see the supporting information for further details of how we produced our filament. Additive manufacturing of the electrodes are detailed in the supporting information, but in summary, all additive-manufactured electrodes were printed using identical printing parameters with a 0.6 mm nozzle, temperature of  $245 \text{ }^\circ\text{C}$  using a 100 % rectilinear infill [17], 0.15 mm layer height and print speed of  $35 \text{ mm s}^{-1}$ . The print bed is set up to be at  $100 \text{ }^\circ\text{C}$ , which is covered with a thin layer of Magigoo® to improve the adherence of PP onto the print bed.

### 2.3. Physicochemical characterisation

X-ray Photoelectron Spectroscopy, Thermogravimetric analysis, Scanning Electron Microscopy (SEM) and Raman are detailed further within the supporting information.

## 2.4. Electrochemical experiments

All electrochemical experiments were performed on an Autolab PGSTAT 204 potentiostat (Utrecht, The Netherlands). Identical additive manufactured electrodes were used throughout this work for all filaments, printed in a lollipop shape ( $\varnothing 5 \text{ mm}$  disc with 8 mm connection length of 2 widths and 1 mm thickness [15]) alongside an external commercial  $\text{Ag}|\text{AgCl}/\text{KCl}$  saturated (3M) reference electrode with a nichrome wire counter electrode. All solutions of  $[\text{Ru}(\text{NH}_3)_6]^{3+}$  were purged of  $\text{O}_2$  thoroughly using  $\text{N}_2$  before any electrochemical experiments. Solutions of  $[\text{Fe}(\text{CN})_6]^{4-/3-}$  were prepared in the same way without the need for further degassing.

Electrochemical impedance spectroscopy (EIS) was recorded in the frequency range 0.1 Hz to 100 kHz applying 10 mV of signal amplitude. NOVA 2.1.7 software was used to fit Nyquist plots obtained to adequate equivalent circuit. The additive-manufactured electrodes were activated before all electrochemical experiments. Please see the supporting information for further details.

## 3. Results and discussion

### 3.1. Preparation and characterisation of graphite and carbon black mixed filament

To overcome some barriers to commercialisation for additive manufacturing electrochemistry, the production of stable, low-cost, yet high-performance filament is required. Previously, the first conductive PP filament has been published, which offers significant improvements in chemical stability and reduction in water ingress. To further improve this and reduce the material costs for production, we follow work previously achieved within PLA by replacing certain proportions of carbon black (CB) with graphite (G). This can dramatically reduce the material cost of production while also improving the sustainability by moving away from petrochemically derived carbons toward a naturally occurring allotrope. As such, compositions replacing different amounts of CB with G were produced and processed into additive manufacturing filament, as described in Fig. 1A. The total loading of carbon within the filament was kept constant at 40 wt%, which was found to be the maximum loading of CB possible to be incorporated within PP filament without the addition of any other additives previously reported.

All the filaments produced offered excellent low-temperature flexibility, Fig. 1B, with no significant reductions as the amount of G incorporated increased. Initially, to establish an indicator of performance and compare to reports within the literature for conductive additive manufacturing filaments, the bulk resistance across 10 cm of filament was measured. The values obtained are presented in Table 1, where it can be seen that the filaments replacing up to 37.5 % of the CB with G produced very similar results to 100 % CB with resistance values between  $170\text{--}191 \Omega$ , while for the 50 % replacement a small increase in resistance up to  $223 \pm 12 \Omega$  was observed and much more significant increases up to  $3367 \pm 163 \Omega$  when the 87.5 % replacement of CB for G was achieved. The resistance values obtained for the filaments up to 50 % replacement show significant improvements on many reported bespoke filaments within the literature and compare well to the most conductive reports of PLA [29]. There are no commercially available conductive PP filaments, but this filament compares excellently to the most commonly used commercial conductive PLA, which has resistance values reported between 2 and 4 k $\Omega$ .

To further evaluate the filaments, they were tested through thermogravimetric analysis to understand how adding these carbon allotropes affected the thermal stability of the filaments, and to confirm that the amount of carbon within the filament was as intended. Fig. 1C shows example outputs from the TGA for each filament produced along with the profile obtained for the virgin PP pellets used. From these plots, the onset of degradation temperature was calculated, showing that the inclusion of carbon materials within the filament offered thermal

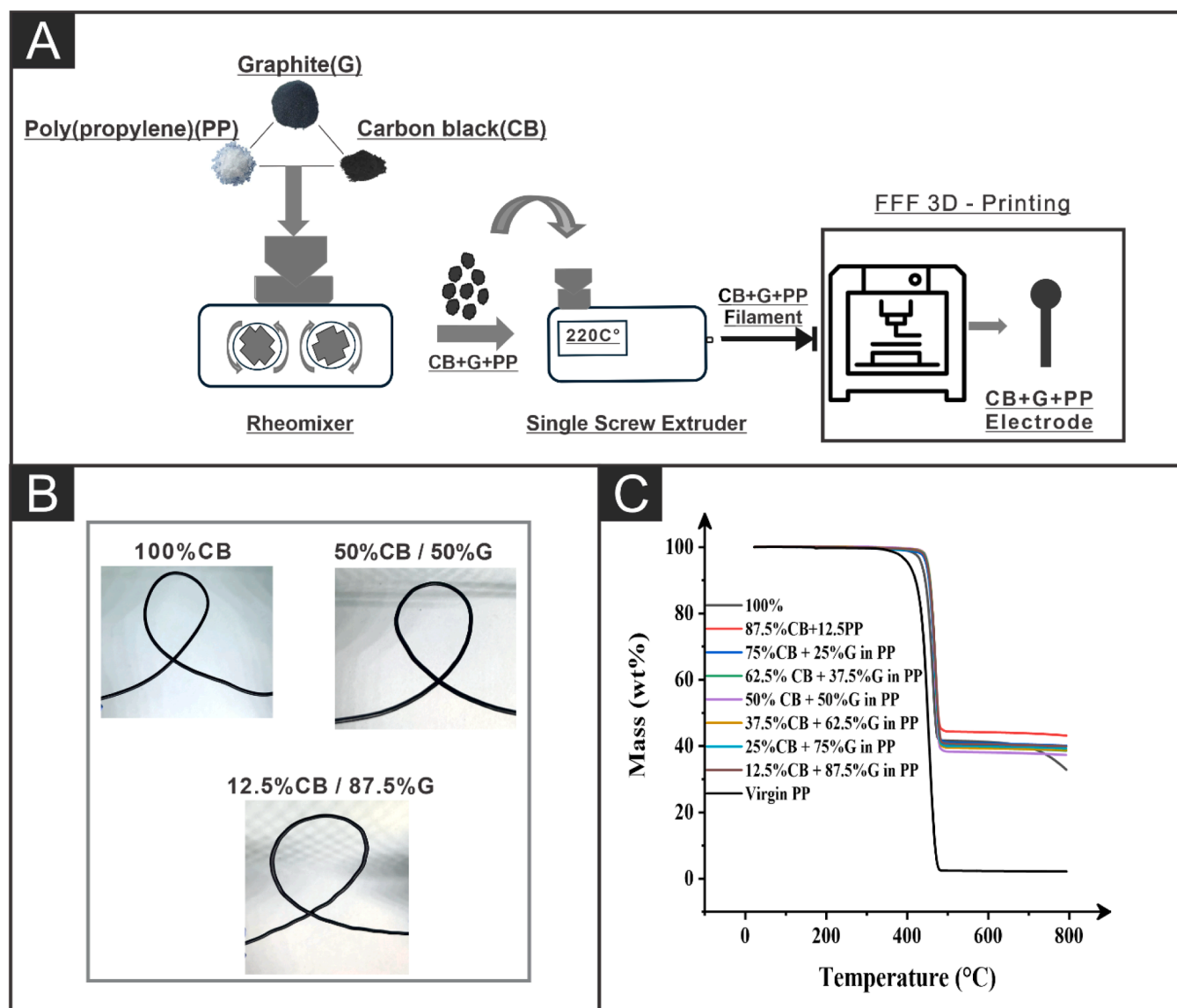


Fig. 1. A) Schematic of filament production. B) Photographs highlighting the low-temperature flexibility of three of the filaments manufactured. C) TGA analysis of the different filaments compared to virgin PP (not containing any conductive filler).

Table 1

Evaluation of the bulk resistance ( $N = 10$ ), onset of degradation temperature, and filler percentage for each bespoke carbon black/graphite filament produced.

| CB: Graphite (%) | Resistance ( $\Omega$ ) | Onset of Degradation ( $^{\circ}\text{C}$ ) | Filler wt% (%) |
|------------------|-------------------------|---|----------------|
| 100: 0           | $172 \pm 21$            | $321 \pm 25$                                | $40 \pm 1$     |
| 87.5: 12.5       | $190 \pm 47$            | $343 \pm 21$                                | $41 \pm 1$     |
| 75: 25           | $177 \pm 4$             | $315 \pm 15$                                | $40 \pm 1$     |
| 62.5: 37.5       | $191 \pm 6$             | $324 \pm 9$                                 | $40 \pm 2$     |
| 50: 50           | $223 \pm 12$            | $389 \pm 5$                                 | $36 \pm 3$     |
| 37.5: 62.5       | $337 \pm 31$            | $379 \pm 17$                                | $37 \pm 1$     |
| 25: 75           | $848 \pm 61$            | $376 \pm 16$                                | $39 \pm 1$     |
| 12.5: 87.5       | $3367 \pm 163$          | $363 \pm 25$                                | $39 \pm 1$     |

stabilisation to the system. From the TGA results, the actual filler content of the filaments was also calculated. All filaments except the 50% and 62.5% graphite filaments aligned with the expected filler content, with these falling slightly below, which needs to be considered regarding the performance in the future.

### 3.2. Electrochemical characterisation of electrodes

Once the eight filaments are produced and characterised, they are used to print electrodes via additive manufacturing (see experimental details) for electrochemical testing. To ensure no warping occurred during the additive manufacturing printing process, specialised glue was deposited onto the additive manufacturing print bed to improve the adhesion. After additive manufacturing printing, the effect of the glue was studied. Fig. 2A presents the cyclic voltammograms obtained in  $[\text{Ru}(\text{NH}_3)_6]^{3+}$  (1 mM in 0.1 M KCl) for additively manufactured electrodes straight from the print bed and cleaned of glue by applying chronoamperometry in NaOH (0.5 M) at +1.4 V for 200 s and -1.0 V for 200 s. A dramatic improvement in the electrochemical response is observed once the electrode is cleaned, whereby the peak-to-peak separation ( $\Delta E_p$ ) improved from  $148 (\pm 3)$  mV to  $93 (\pm 18)$  mV. This indicated that the glue deposited on the bed remains on the surface of the electrode, creating a layer thick enough to inhibit the electron transfer process, for even near-ideal outer sphere probes. Therefore, for all remaining electrochemical experiments, all of the electrodes via additive manufacturing are cleaned using the protocol above before use.

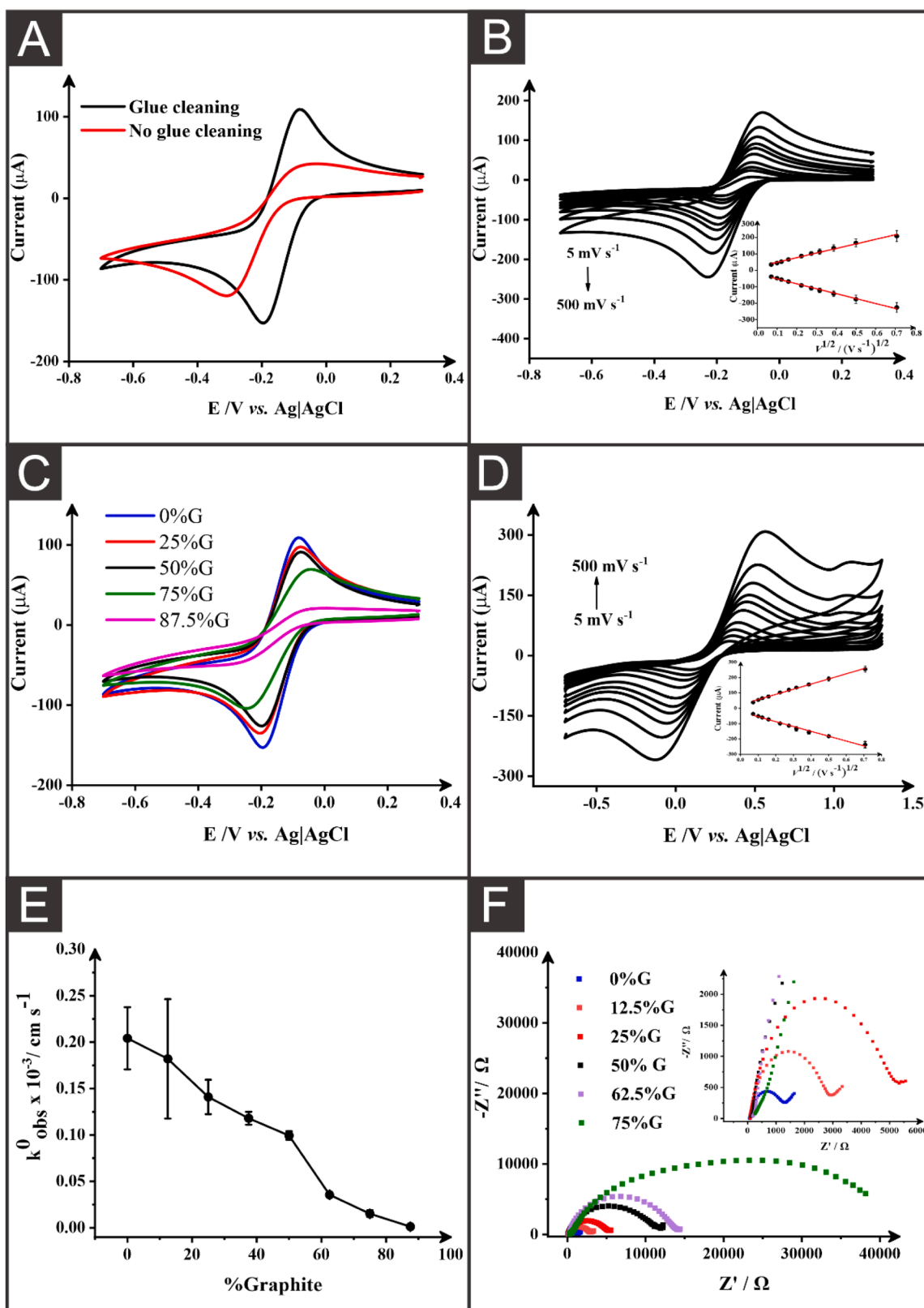


**Fig. 2.** A) Typical cyclic voltammograms (100 mV s<sup>-1</sup>) of [Ru(NH<sub>3</sub>)<sub>6</sub>]<sup>3+</sup> (1 mM in 0.1 M KCl) with the CB-G-PP filament using additive manufactured electrodes with a counter electrode of nickel/chrome and a Ag/AgCl as reference electrode for the cleaned electrode (black voltammogram) and not cleaned electrode (red voltammogram). B) Typical cyclic voltammograms showing a scan rate study (5–500 mV s<sup>-1</sup>) of [Ru(NH<sub>3</sub>)<sub>6</sub>]<sup>3+</sup> (1 mM in 0.1 M KCl) with the 50:50 CB-G-PP additive manufactured electrode. C) Comparison (100 mV s<sup>-1</sup>) of 0% G, 25% G, 50% G, 75% G and 87.5% G additive manufactured electrodes using the outer-sphere redox probe [Ru(NH<sub>3</sub>)<sub>6</sub>]<sup>3+</sup> (1 mM in 0.1 M KCl). D) An example of scan rate study using 50:50 CB-G-PP additive manufactured electrode using the inner-sphere redox probe [Fe(CN)<sub>6</sub>]<sup>4-</sup>. E) A plot of the heterogeneous rate constant,  $k_{obs}^0$  versus the % graphite using the inner-sphere probe [Fe(CN)<sub>6</sub>]<sup>4-</sup>. F) EIS Nyquist plots for all bespoke carbon black/graphite electrodes.



As shown, scan rate studies (5–500 mV s<sup>-1</sup>) are then performed using additive manufacturing electrodes printed from all the filaments produced after cleaning. An example of the cyclic voltammograms obtained within [Ru(NH<sub>3</sub>)<sub>6</sub>]<sup>3+</sup> (1 mM in 0.1 M KCl) using the 50:50 CB-G-PP additive manufactured electrode are shown within Fig. 2B. This was chosen as [Ru(NH<sub>3</sub>)<sub>6</sub>]<sup>3+</sup> is a near-ideal outer sphere redox probe and therefore, allows for the best determination of the heterogeneous electron (charge) transfer rate constant ( $k_{obs}^0$ ) and the real electrochemical surface area ( $A_{real}$ ) [40]. A summary of the key pieces of data obtained from this study can be found within Table 2, with a comparison between cyclic voltammograms obtained at the same scan rate shown within Fig. 2C. Toward this probe, there was no significant decrease in performance upon the inclusion of graphite up to 62.5 %, where comparing this with the 100 % CB filament they produced peak cathodic currents ( $I_{pc}$ ) of 127 (± 20) μA and 124 (± 30) μA,  $\Delta E_p$  values of 96 (± 4) mV and 93 (± 18) mV,  $k_{obs}^0$  values of 1.85 (± 0.05) × 10<sup>-3</sup> cm s<sup>-1</sup> and 1.91 (± 0.20) × 10<sup>-3</sup> cm s<sup>-1</sup>, and  $A_{real}$  values of 0.56 (± 0.10) cm<sup>2</sup> and 0.57 (± 0.06) cm<sup>2</sup> respectively. Once the ratio of graphite increased to 75 % and 87.5 % there began to be significant decreases in the electrochemical performance, with the 87.5 % filament producing an  $I_{pc}$  of 51 (± 3) μA, a  $\Delta E_p$  of 208 (± 4) mV, a  $k_{obs}^0$  of 0.52 (± 0.06) × 10<sup>-3</sup> cm s<sup>-1</sup>, and an  $A_{real}$  of 0.27 (± 0.01) cm s<sup>-1</sup>.

These trends were clear against [Ru(NH<sub>3</sub>)<sub>6</sub>]<sup>3+</sup>, however, the majority of electroanalytical targets are not near-ideal outer sphere probes. As such, it is essential to characterise electrode materials toward inner sphere probes. To this end, we evaluated additive manufactured electrodes from all 8 filaments against the commonly used probe [Fe(CN)<sub>6</sub>]<sup>4-</sup> (1 mM in 0.1 M KCl). Fig. 2D shows an example of the obtained scan rate study (5–500 mV s<sup>-1</sup>) using the 50:50 CB-G-PP electrode. Through these plots, a  $k^0$  for each of the 8 filaments was produced, which is plotted in Fig. 2E. It can be seen that the  $k^0$  decreases for increased amounts of graphite with a larger decrease from 0.10 (± 0.04) × 10<sup>-3</sup> cm s<sup>-1</sup> for 50 % to 0.04 (± 0.02) × 10<sup>-3</sup> cm s<sup>-1</sup> for 62.5 % graphite. The performance of these electrodes was further tested by electrochemical impedance spectroscopy (EIS). Through fitting of the obtained Nyquist plots with the appropriate Randles circuit, the solution resistance ( $R_s$ ) and the charge-transfer resistance ( $R_{CT}$ ) were calculated. Fig. 2F shows the obtained Nyquist plots, with a magnified inset, and the calculated  $R_s$  and  $R_{CT}$  values are summarised within Table 2. There is an apparent increase in both the  $R_s$  and  $R_{CT}$  values as the loading of graphite increased within

**Table 2**

Summary of the electrochemical results obtained for the testing of filaments, including the cathodic peak current ( $I_{pc}$ ) and peak-to-peak separation ( $\Delta E_p$ ), heterogeneous electron (charge) transfer rate constant ( $k_{obs}^0$ ), all calculated from cyclic voltammograms using [Ru(NH<sub>3</sub>)<sub>6</sub>]<sup>3+</sup> (1 mM in 0.1 M KCl). Additionally, the solution resistance ( $R_s$ ) and charge-transfer resistance ( $R_{CT}$ ) from EIS in [Fe(CN)<sub>6</sub>]<sup>4-3-</sup> (1 mM in 0.1 M KCl).

| CB: Graphite (%) | $I_{pc}$ (μA) | $\Delta E_p$ (mV) | $k_{obs}^0$ (x 10 <sup>-3</sup> cm s <sup>-1</sup> ) | $A_{real}$ (cm <sup>2</sup> ) | $R_s$ (Ω) | $R_{CT}$ (kΩ) |
|------------------|---------------|-------------------|--|-------------------------------|-----------|---------------|
| 100: 0           | 124 ± 30      | 93 ± 18           | 1.91 ± 0.20  | 0.56 ± 0.10                   | 74 ± 1    | 1.92 ± 0.7    |
| 87.5: 12.5       | 114 ± 20      | 84 ± 8            | 2.21 ± 0.10  | 0.45 ± 0.09                   | 81 ± 3    | 2.37 ± 0.4    |
| 75: 25           | 132 ± 13      | 99 ± 19           | 1.95 ± 0.30  | 0.55 ± 0.03                   | 80 ± 7    | 3.07 ± 0.7    |
| 62.5: 37.5       | 82 ± 3        | 113 ± 9           | 1.52 ± 0.11  | 0.46 ± 0.02                   | 85 ± 4    | 3.37 ± 0.7    |
| 50: 50           | 122 ± 14      | 83 ± 13           | 2.08 ± 0.22  | 0.49 ± 0.05                   | 151 ± 41  | 7.05 ± 0.7    |
| 37.5: 62.5       | 127 ± 20      | 96 ± 4            | 1.85 ± 0.05  | 0.57 ± 0.06                   | 239 ± 65  | 18.9 ± 0.7    |
| 25: 75           | 110 ± 19      | 133 ± 3           | 1.09 ± 0.06  | 0.44 ± 0.07                   | -         | -             |
| 12.5: 87.5       | 51 ± 3        | 208 ± 4           | 0.52 ± 0.06  | 0.27 ± 0.01                   | -         | -             |

the sample. Note that use of the outer-sphere redox probe [Ru(NH<sub>3</sub>)<sub>6</sub>]<sup>3+</sup> has reported a value of  $k_{obs}^0$  of 4.57 × 10<sup>-4</sup> cm s<sup>-1</sup> for the conductive commercial carbon black with PLA (ProtoPasta) [37] which shows that our filament provides an electrochemically attractive electrode surface via additive manufacturing. Clearly, if the goal is to create the optimal filament for electrochemical performance from this selection, the 100 % CB would be the choice. However, the addition of graphite is important for the reduction in material costs. It is important to note that differences in material cost will depend on the quality of materials and suppliers used, however for the purpose of this work we utilised readily available and well-tested sources of CB and G. The respective costs were £0.26 per gram of CB and £0.06 per gram of G. As such, every part of CB replaced with G offers significant cost savings and therefore a balance and compromise must be struck for each intended end use. In our case we are looking for a good electrochemical performance with high-cost savings as proof-of-concept. Thus, from the data obtained and observing Table 2, there is clearly good electrochemical performance up to 50 % G inclusion, however for EIS this filament does not perform as well as the 37.5 % G inclusion sample. The material cost for producing a 1 kg spool of these filaments was calculated at £63.20 and £73.40 respectively, and therefore even though there was a slight drop in electrochemical performance the 50 % G filament was chosen for further studies. Using these material costs and the electrode designs in this work, we calculate that the cost per electrode is <1 p (£0.0076), meaning that thousands of electrodes could be printed for less cost than purchasing some commercial electrodes. The combination of graphite flakes with a lower concentration of smaller particles is believed to reduce the electrically conductive network within the polymer, thereby reducing conductivity and as shown, a reduction in the heterogeneous rate constant; when the concentration of large flakes becomes excessive, the dispersed graphite fails to establish sufficient connections, resulting in a suboptimal conductive network.

### 3.3. Physicochemical characterisation of the selected 50:50 CB/G electrodes

Once decided upon, exploring the physicochemical properties of the additively manufactured electrodes produced from the 50 % CB-50 %G-PP filaments was important. Fig. 3A presents the C 1 s spectra obtained for the activated electrode, and Fig. 3B the as-printed electrode. For the production of an adequate fit, three peaks must be assigned. Firstly, there is an asymmetric peak fitted at 284.5 eV, assigned to graphitic carbon's X-ray photoemission [41,42]. Two additional symmetric peaks were then required for fitting corresponding to the sp<sup>3</sup> C-C and the C=O bonding present. The more significant intensity of C-C bonding is expected due to the structure of PP and the carbon fillers, with C=O bonding attributed to functionalities on the surface of both the CB and G. This fitting produced an excellent standard deviation of 1.33 and was used to estimate the atomic concentrations of these different functionalities, with 44 % attributed to the sp<sup>2</sup> graphitic carbon, 55 % to the sp<sup>3</sup> C-C bonding and 1 % to the C=O bonding.

Raman spectroscopy, Fig. 3C and D, showed well-defined peaks at 1338, 1572, and 2680 cm<sup>-1</sup>. These were attributed to the characteristic D-, G-, and 2D bands found within the expected Raman spectra for graphitic structures. It can be seen that the intensity of these peaks varies significantly, which stems from the mixture of CB and G. Through the calculation of the I<sub>D</sub>/I<sub>G</sub> band ratio for each spectrum we can see that when the laser during Raman analysis hits CB, as in Fig. 3C, a value of 1.075 is calculated. In contrast, for a flake of graphite in Fig. 3D which is evident from electrochemical activation, we obtain 0.038, confirming the increase in order of the graphite structure. The surface of the electrodes was then imaged through SEM, where micrographs at 5k, and 25k magnification are shown within Fig. 3E and F, respectively. On the surface of the electrodes, it can be seen that there is a polymer covering with significant amounts of small perforations, allowing access to the conductive filler beneath. Although there is no sign of CB on the surface,

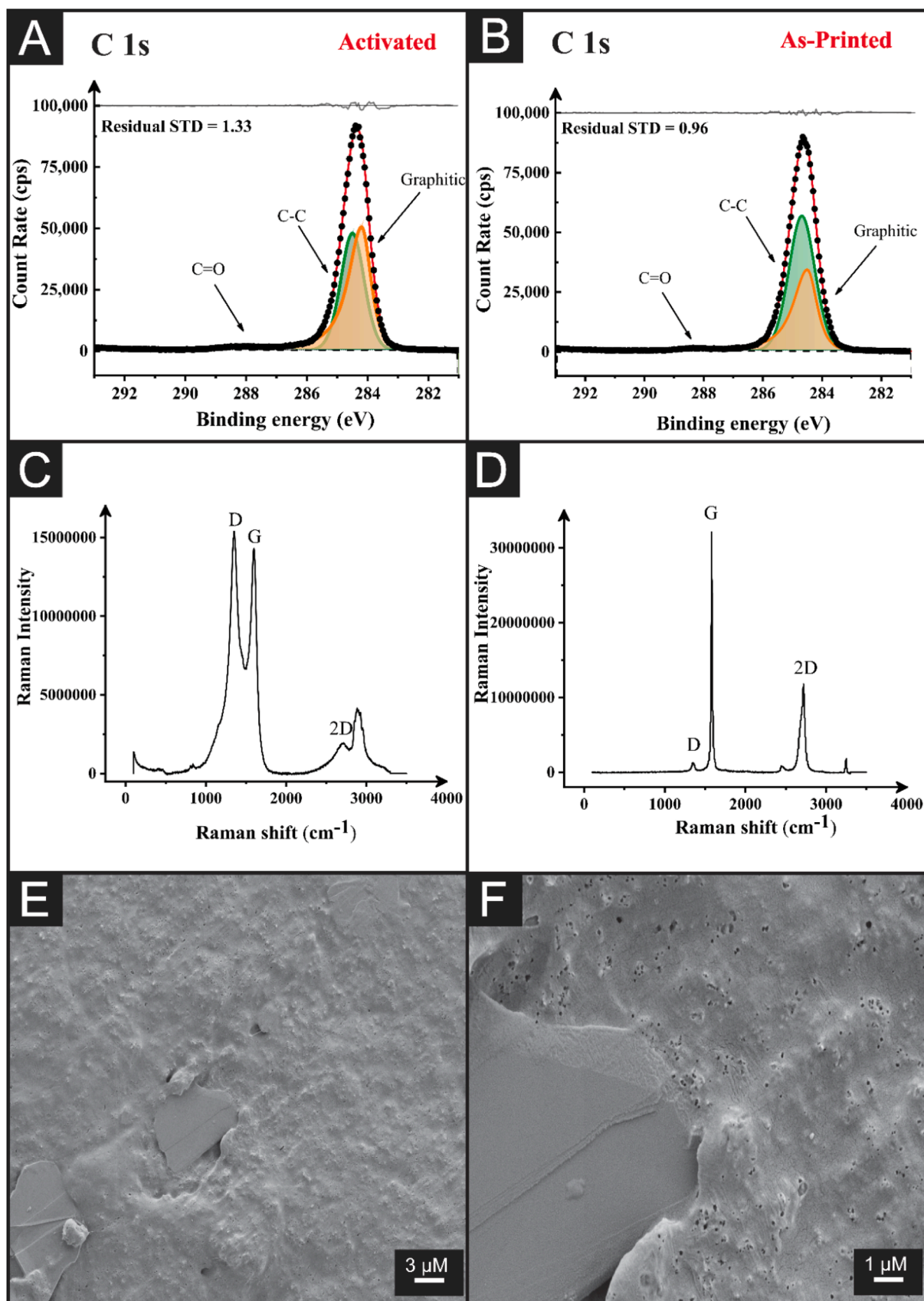


**Fig. 3.** A) XPS spectra for activated 50 % CB-50 % G-PP electrode showing the C 1s region and B) as-printed 50 %CB-50 %G-PP electrode showing C 1s. Raman spectra obtained for 50 %CB-50 % G as printed electrode C) and 50 %–50 %G-PP activated electrode D). SEM images for additive manufactured electrodes following activation at E) 5k and F) 25k magnification.

raised spherical lumps in the polymer layer indicate the presence of CB below. Additionally, a visible graphite flake protrudes from the surface of the polymer.

### 3.4. Detection of chlorpromazine in acetonitrile

Once the physicochemical characteristics of the additive manufacturing electrodes are investigated, we will explore the use of this electrode within organic electroanalysis, a yet unexplored field within additive manufacturing electrochemistry. In this regard, we look to utilise the beneficial chemical stability of PP to progress in this field and provide proof of concept by detecting the presence of chlorpromazine in acetonitrile using the bespoke CB-G-PP filament. Chlorpromazine is an antipsychotic drug used in the treatment of schizophrenia and

related psychoses [43,44]. Fig. 4A shows the quasi-reversible cyclic voltammetric scan rate study ( $5\text{--}500\text{ mV s}^{-1}$ ) for chlorpromazine (0.1 mM, 0.1 M tetrabutylammonium perchlorate (TBAP) in MeCN), with inset of Fig. 4A, Randles-Ševčík plot are shown which confirms the electrochemical oxidation of chlorpromazine is a diffusion-controlled process. Furthermore, the use of the Laviron equation suggest that this process involves the transfer of one electron. This work agrees with the use of multiwalled carbon nanotubes and a Thiocalix[4]arene-based Metal-Organic Framework; [45] a tentative mechanism is shown in the Scheme S1 which suggests that one electron is transferred, making chlorpromazine into a radical cation. The second minor peak is evident within Fig. 4C which suggests that the product is inconsequentially adsorbed; further work is underway on the electrochemical mechanism. Fig. 4B shows the cyclic voltammograms ( $100\text{ mV s}^{-1}$ ) for the 50 %-G

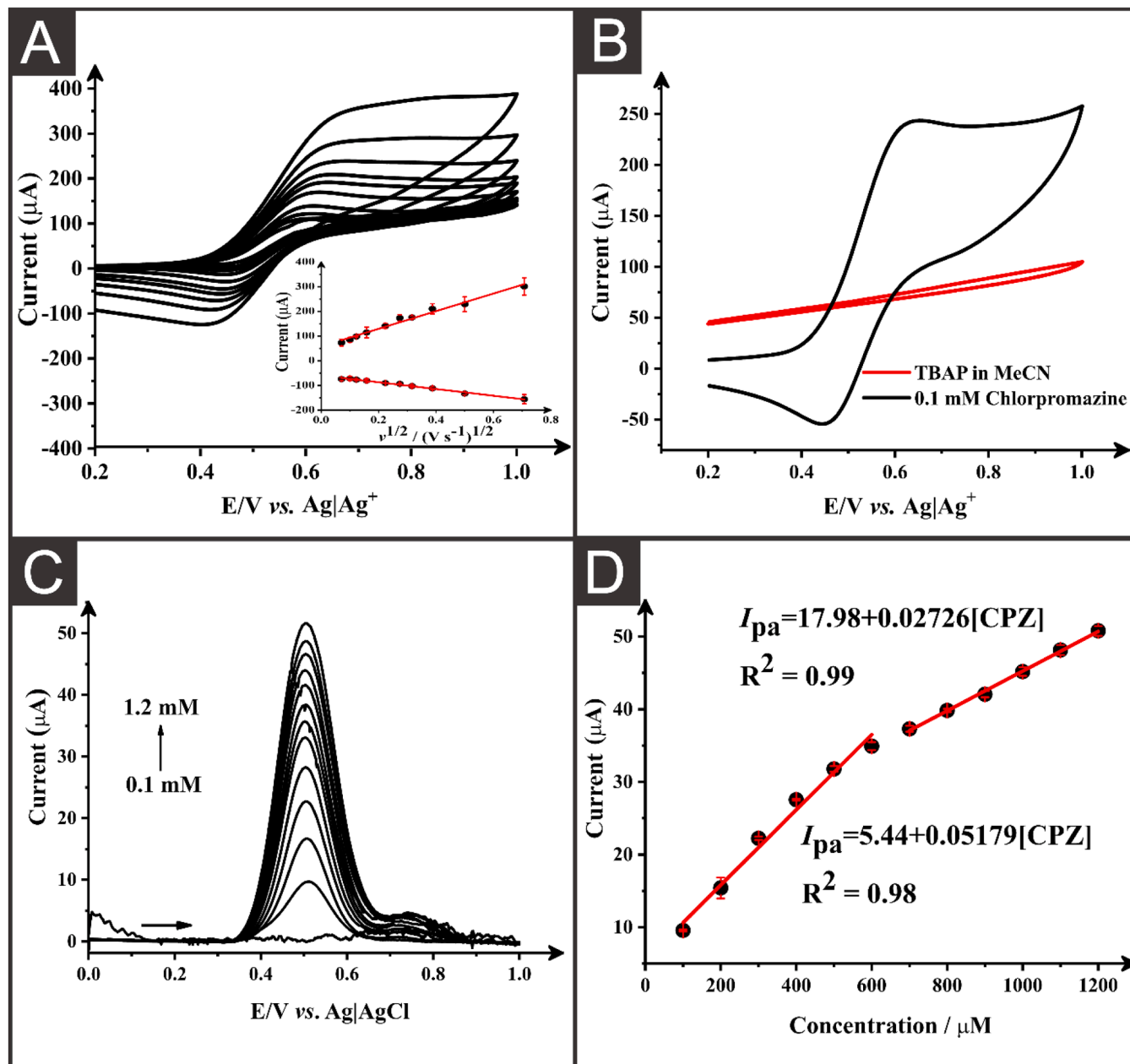


Fig. 4. A) Scan rate study ( $5\text{--}500\text{ mV s}^{-1}$ ) for chlorpromazine (0.1 mM in 0.1 M tetrabutylammonium perchlorate (TBAP) in MeCN) with the 50:50 CB-G-PP electrode as the WE, nickel/chrome as CE and  $\text{Ag}/\text{Ag}^+$  (0.01 M  $\text{AgNO}_3$ , 0.1 M TBAP/MeCN) as RE. B) Comparison of the cyclic voltammograms obtained at  $100\text{ mV s}^{-1}$  for presence and absence of chlorpromazine (0.1 mM in 0.1 M TBAP in MeCN) using 50:50 CB-G-PP electrode. C) Differential pulse voltammetry of increasing concentration of chlorpromazine between 0.1 mM - 2 mM measured in 0.1 M TBAP in MeCN using 50:50 CB-G-PP electrode and the corresponding calibration plot are shown in D); the average is shown with the standard deviation using 5 repeats. Each calibration run are performed using the same electrode .



filament with, and without, the presence of chlorpromazine (0.1 mM) in 0.1 M TBAP and MeCN; clear oxidation and reduction peaks can be observed for the one-electron processes, with a  $\Delta E_p$  of 170 mV.

The detection of chlorpromazine within MeCN are next studied using differential pulse voltammetry with the results between 0.1–1.2 mM shown in Fig. 4C. The optimised method for the differential pulse voltammetry technique was obtained from the work of Tajik et al. [46] This data was used to create an appropriate calibration plot, Fig. 4D, which produced two linear lines of detection. The first line between 0.1–0.6 mM had a sensitivity of  $51.8 \text{ nA } \mu\text{M}^{-1}$  and produced a limit of detection of  $80 \text{ } \mu\text{M}$  and limit of quantification of  $266 \text{ } \mu\text{M}$ . This work provides a proof of concept for conductive poly(propylene) based filament unlocking the door to organic electroanalysis. We believe this has scope to drive the wider uptake of additive manufacturing electrochemistry, where low-cost but high-performance electrodes can be quickly and easily produced on site.

#### 4. Conclusions

In this work, we report the first production of an optimised low-cost conductive poly(propylene) based filament for additive manufacturing electrochemistry. Through optimising the loading ratio between carbon black and graphite, we reduced the material cost of a 1 kg spool of material by  $>£40$ . Using a filament containing equal amounts of graphite and carbon black, electrodes could be printed for less than £0.01 each. These electrodes were characterised physicochemically and electrochemically, showing excellent performance. The material was then applied to detect chlorpromazine within acetonitrile, unlocking the door to organic electroanalysis. This area of research has been previously unobtainable for additive manufacturing electrochemistry. Using these electrodes, a sensitivity of  $51.8 \text{ nA } \mu\text{M}^{-1}$ , LOD of  $80 \text{ } \mu\text{M}$ , and LOQ of  $266 \text{ } \mu\text{M}$  are obtained. This work shows how low-cost, chemically stable electrodes can be manufactured rapidly on-site and unlock the door for additive manufacturing electrochemistry to enter new fields within the realms of organic media.

#### Supporting information

Pictures of filaments; Relation of resistance ( $\Omega$ ) and % of graphite; Pictures of electrodes; Relation of  $k_{obs}^0$  and % of graphite; electrochemical mechanism.

#### CRedit authorship contribution statement

**Bruno Ferreira:** Formal analysis, Investigation, Methodology, Writing – original draft, Writing – review & editing. **Robert D. Crapnell:** Methodology, Supervision, Writing – original draft, Writing – review & editing. **Elena Bernalte:** Investigation, Methodology, Supervision, Writing – original draft, Writing – review & editing. **Thiago R.L.C. Paixão:** Writing – original draft, Writing – review & editing, Funding acquisition, Supervision. **Craig E. Banks:** Conceptualization, Formal analysis, Funding acquisition, Project administration, Resources, Supervision, Writing – original draft, Writing – review & editing.

#### Declaration of competing interest

The authors declare that they have no known competing financial interests or personal relationships that could have appeared to influence the work reported in this paper.

#### Acknowledgements

This research was supported by Horizon Europe grant 101137990, São Paulo Research Foundation (FAPESP) (Grant number: 2023/00246-1), Coordenação de Aperfeiçoamento de Pessoal de Nível Superior - Brasil (CAPES) (Grant numbers: 88887.601733/2021-00 and Finance

Code 001), Conselho Nacional de Desenvolvimento Científico e Tecnológico (Grant number: 405620/2021-7, 465389/2014-7 and 302839/2020-8).

#### Supplementary materials

Supplementary material associated with this article can be found, in the online version, at doi:10.1016/j.electacta.2025.145680.

#### Data availability

Data will be made available on request.

#### References

- [1] A. Abdalla, B.A. Patel, 3D printed electrochemical sensors, *Annu. Rev. Anal. Chem.* 14 (2021) 47–63.
- [2] A. Abdalla, B.A. Patel, 3D-printed electrochemical sensors: a new horizon for measurement of biomolecules, *Curr. Opin. Electrochem.* 20 (2020) 78–81.
- [3] R.M. Cardoso, C. Kalinke, R.G. Rocha, P.L. Dos Santos, D.P. Rocha, P.R. Oliveira, B. C. Janegitz, J.A. Bonacin, E.M. Richter, R.A. Munoz, Additive-manufactured (3D-printed) electrochemical sensors: a critical review, *Anal. Chim. Acta* 1118 (2020) 73–91.
- [4] R.D. Crapnell, E. Bernalte, A.G.-M. Ferrari, M.J. Whittingham, R.J. Williams, N. J. Hurst, C.E. Banks, All-in-one single-print additively manufactured electroanalytical sensing platforms, *ACS Meas. Sci. Au* 2 (2021) 167–176.
- [5] B.C. Janegitz, R.D. Crapnell, P. Roberto de Oliveira, C. Kalinke, M.J. Whittingham, A. Garcia-Miranda Ferrari, C.E. Banks, Novel Additive manufactured multielectrode electrochemical cell with honeycomb inspired design for the detection of methyl parathion in honey samples, *ACS Meas. Sci. Au* 3 (2023) 217–225.
- [6] V. Adimule, N. Manhas, S. Nandi, Additively Manufactured Electrochemical and Biosensors, *Practical Implementations of Additive Manufacturing Technologies*, Springer, 2023, pp. 191–204.
- [7] R.D. Crapnell, C.E. Banks, Electroanalysis overview: additive manufactured biosensors using fused filament fabrication, *Anal. Methods* 16 (2024) 2625–2634.
- [8] J. Muñoz, M. Pumera, 3D-printed biosensors for electrochemical and optical applications, *TrAC Trends Anal. Chem.* 128 (2020) 115933.
- [9] M.P. Browne, E. Redondo, M. Pumera, 3D printing for electrochemical energy applications, *Chem. Rev.* 120 (2020) 2783–2810.
- [10] K. Ghosh, S. Ng, C. Iffelsberger, M. Pumera, 2D MoS<sub>2</sub>/carbon/poly(lactic acid) filament for 3D printing: photo and electrochemical energy conversion and storage, *Appl. Mater. Today* 26 (2022) 101301.
- [11] K. Ghosh, M. Pumera, Free-standing electrochemically coated MoS<sub>x</sub> based 3D-printed nanocarbon electrode for solid-state supercapacitor application, *Nanoscale* 13 (2021) 5744–5756.
- [12] K. Ghosh, M. Pumera, MXene and MoS<sub>3-x</sub> coated 3D-printed hybrid electrode for solid-state asymmetric supercapacitor, *Small Methods* 5 (2021) 2100451.
- [13] M.J. Whittingham, R.D. Crapnell, E.J. Rothwell, N.J. Hurst, C.E. Banks, Additive manufacturing for electrochemical labs: an overview and tutorial note on the production of cells, electrodes and accessories, *Talanta Open* 4 (2021) 100051.
- [14] M.J. Whittingham, R.D. Crapnell, C.E. Banks, Additively manufactured rotating disk electrodes and experimental setup, *Anal. Chem.* 94 (2022) 13540–13548.
- [15] R.D. Crapnell, A. Garcia-Miranda Ferrari, M.J. Whittingham, E. Sigley, N.J. Hurst, E.M. Keefe, C.E. Banks, Adjusting the connection length of additively manufactured electrodes changes the electrochemical and electroanalytical performance, *Sensors* 22 (2022) 9521.
- [16] A.G.-M. Ferrari, N.J. Hurst, E. Bernalte, R.D. Crapnell, M.J. Whittingham, D. A. Brownson, C.E. Banks, Exploration of defined 2-dimensional working electrode shapes through additive manufacturing, *Analyst* 147 (2022) 5121–5129.
- [17] E. Bernalte, R.D. Crapnell, O.M. Messai, C.E. Banks, The effect of slicer infill pattern on the electrochemical performance of additively manufactured electrodes, *ChemElectroChem* 11 (2024) e202300576.
- [18] R. Shergill, B. Patel, The effects of material extrusion printing speed on the conductivity of carbon black/poly(lactic acid) electrodes, (2022).
- [19] R.S. Shergill, C.L. Miller, B.A. Patel, Influence of instrument parameters on the electrochemical activity of 3D printed carbon thermoplastic electrodes, *Sci. Rep.* 13 (2023) 339.
- [20] R.S. Shergill, B.A. Patel, The effects of material extrusion printing speed on the electrochemical activity of carbon black/poly(lactic acid) electrodes, *ChemElectroChem* 9 (2022) e202200831.
- [21] C. Iffelsberger, C.W. Jellett, M. Pumera, 3D printing temperature tailors electrical and electrochemical properties through changing inner distribution of graphite/polymer, *Small* 17 (2021) 2101233.
- [22] C. Kalinke, N.V. Neumsteir, G. de Oliveira Aparecido, T.V. de Barros Ferraz, P. L. Dos Santos, B.C. Janegitz, J.A. Bonacin, Comparison of activation processes for 3D printed PLA-graphene electrodes: electrochemical properties and application for sensing of dopamine, *Analyst* 145 (2020) 1207–1218.
- [23] D.P. Rocha, R.G. Rocha, S.V. Castro, M.A. Trindade, R.A. Munoz, E.M. Richter, L. Angnes, Posttreatment of 3D-printed surfaces for electrochemical applications: a critical review on proposed protocols, *Electrochem. Sci. Adv.* 2 (2022) e2100136.

- [24] R.S. Shergill, B.A. Patel, Preprinting saponification of carbon thermoplastic filaments provides ready-to-use electrochemical sensors, *ACS Appl. Electron. Mater.* 5 (2023) 5120–5128.
- [25] R.S. Shergill, F. Perez, A. Abdalla, B.A. Patel, Comparing electrochemical pre-treated 3D printed native and mechanically polished electrode surfaces for analytical sensing, *J. Electroanal. Chem.* 905 (2022) 115994.
- [26] R.D. Crapnell, C. Kalinke, L.R.G. Silva, J.S. Stefano, R.J. Williams, R.A.A. Munoz, J.A. Bonacin, B.C. Janegitz, C.E. Banks, Additive manufacturing electrochemistry: an overview of producing bespoke conductive additive manufacturing filaments, *Mater. Today* 71 (2023) 73–90.
- [27] I.V. Arantes, R.D. Crapnell, M.J. Whittingham, E. Sigley, T.R. Paixão, C.E. Banks, Additive manufacturing of a portable electrochemical sensor with a recycled conductive filament for the detection of atropine in spiked drink samples, *ACS Appl. Eng. Mater.* 1 (2023) 2397–2406.
- [28] P. Wuamprakhon, R.D. Crapnell, E. Sigley, N.J. Hurst, R.J. Williams, M. Sawangphruk, E.M. Keefe, C.E. Banks, Recycled additive manufacturing feedstocks for fabricating high voltage, low-cost aqueous supercapacitors, *Adv. Sustain. Syst.* 7 (2023) 2200407.
- [29] R.D. Crapnell, I.V. Arantes, J.R. Camargo, E. Bernalte, M.J. Whittingham, B.C. Janegitz, T.R. Paixão, C.E. Banks, Multi-walled carbon nanotubes/carbon black/rPLA for high-performance conductive additive manufacturing filament and the simultaneous detection of acetaminophen and phenylephrine, *Microchim. Acta* 191 (2024) 96.
- [30] C. Kalinke, R.D. Crapnell, E. Sigley, M.J. Whittingham, P.R. de Oliveira, L.C. Brazaca, B.C. Janegitz, J.A. Bonacin, C.E. Banks, Recycled additive manufacturing feedstocks with carboxylated multi-walled carbon nanotubes toward the detection of yellow fever virus cDNA, *Chem. Eng. J.* 467 (2023) 143513.
- [31] I.V. Arantes, R.D. Crapnell, E. Bernalte, M.J. Whittingham, T.R. Paixão, C.E. Banks, Mixed graphite/carbon black recycled PLA conductive additive manufacturing filament for the electrochemical detection of oxalate, *Anal. Chem.* 95 (2023) 15086–15093.
- [32] K.K. Augusto, R.D. Crapnell, E. Bernalte, S. Zighed, A. Ehamparanathan, J.L. Pimlott, H.G. Andrews, M.J. Whittingham, S.J. Rowley-Neale, O. Fatibello-Filho, Optimised graphite/carbon black loading of recycled PLA for the production of low-cost conductive filament and its application to the detection of  $\beta$ -estradiol in environmental samples, *Microchim. Acta* 191 (2024) 375.
- [33] E. Sigley, C. Kalinke, R.D. Crapnell, M.J. Whittingham, R.J. Williams, E.M. Keefe, B.C. Janegitz, J.A. Bonacin, C.E. Banks, Circular economy electrochemistry: creating additive manufacturing feedstocks for caffeine detection from post-industrial coffee pod waste, *ACS Sustain. Chem. Eng.* 11 (2023) 2978–2988.
- [34] R.D. Crapnell, I.V. Arantes, M.J. Whittingham, E. Sigley, C. Kalinke, B.C. Janegitz, J.A. Bonacin, T.R. Paixão, C.E. Banks, Utilising bio-based plasticiser castor oil and recycled PLA for the production of conductive additive manufacturing feedstock and detection of bisphenol A, *Green Chem.* 25 (2023) 5591–5600.
- [35] K.S. Erokhin, E.G. Gordeev, V.P. Ananikov, Revealing interactions of layered polymeric materials at solid-liquid interface for building solvent compatibility charts for 3D printing applications, *Sci. Rep.* 9 (2019) 20177.
- [36] R.J. Williams, T. Brine, R.D. Crapnell, A.G.-M. Ferrari, C.E. Banks, The effect of water ingress on additively manufactured electrodes, *Mater. Adv.* 3 (2022) 7632–7639.
- [37] J.R. Camargo, R.D. Crapnell, E. Bernalte, A.J. Cunliffe, J. Redfern, B.C. Janegitz, C.E. Banks, Conductive recycled PETg additive manufacturing filament for sterilisable electroanalytical healthcare sensors, *Appl. Mater. Today* 39 (2024) 102285.
- [38] R.D. Crapnell, E. Bernalte, E. Sigley, C.E. Banks, Recycled PETg embedded with graphene, multi-walled carbon nanotubes and carbon black for high-performance conductive additive manufacturing feedstock, *RSC Adv.* 14 (2024) 8108–8115.
- [39] D. Ramos, R. Crapnell, R. Asra, E. Bernalte, A. Oliveria, R. Munoz, E. Richter, A.M. Jones, C.E. Banks, Conductive polypropylene additive manufacturing feedstock: application to aqueous electroanalysis and unlocking non-aqueous electrochemistry and electrosynthesis, *ACS Appl. Mater. Interfaces* (2024).
- [40] R.D. Crapnell, C.E. Banks, Perspective: what constitutes a quality paper in electroanalysis? *Talanta Open* 4 (2021) 100065.
- [41] R. Blume, D. Rosenthal, J.P. Tessonnier, H. Li, A. Knop-Gericke, R. Schlögl, Characterizing graphitic carbon with X-ray photoelectron spectroscopy: a step-by-step approach, *ChemCatChem* 7 (2015) 2871–2881.
- [42] T.R. Gengenbach, G.H. Major, M.R. Linford, C.D. Easton, Practical guides for x-ray photoelectron spectroscopy (XPS): interpreting the carbon 1s spectrum, *J. Vac. Sci. Technol. A* 39 (2021).
- [43] R. Asra, A.M. Jones, Green electrosynthesis of drug metabolites, *Toxicol. Res. (Camb)* 12 (2023) 150–177.
- [44] B. Thornley, J. Rathbone, C. Adams, G. Awad, Chlorpromazine versus placebo for schizophrenia, *Cochrane Database Syst. Rev.* 2 (2003).
- [45] L. Ma, W.-Y. Pei, J. Yang, J.-F. Ma, Efficient electrochemical sensing of chlorpromazine with a composite of multiwalled carbon nanotubes and a thiacalix [4]arene-based metal-organic framework, *Langmuir* 40 (2024) 17656–17666.
- [46] S. Tajik, H. Beitollahi, A sensitive chlorpromazine voltammetric sensor based on graphene oxide modified glassy carbon electrode, *Anal. Bioanal. Chem. Res.* 6 (2019) 171–182.